PROCEEDINGS OF SCIENCE

Study of the $e^+e^- \to p\overline{p}$ process at *BABAR*

David R. Muller* **for the *BABAR* collaboration**
SLAC National Accelerator Laboratory
E-mail: muller@slac.stanford.edu

Low-energy e^+e^- annihilation processes are accessible at *BABAR* via initial state radiation. The $e^+e^- \to p\overline{p}$ cross section is measured over a wide energy range from production threshold up to 4.5 GeV, using a data set of 469 fb^{-1}. The proton magnetic form factor and the ratio of the electric to magnetic form factors are extracted from the measured cross section and angular distribution, respectively, with unprecedented accuracy. The steep rise of the form factor at energies close to the production threshold, as well as unexplained structures at higher energies are confirmed.

XXI International Workshop on Deep-Inelastic Scattering and Related Subject -DIS2013,
22-26 April 2013
Marseilles,France

*Speaker.

PoS(DIS 2013)161

1. Introduction

We present a study [1] of electron-positron annihilations into the proton-antiproton final state using the tagged initial-state radiation (ISR) technique at *BABAR*. This study is based on our full data sample and supersedes our previous measurement [2], which used roughly half the data.

The cross section for the 2→2 body annihilation process $e^+e^- \to p\overline{p}$ can be expressed as

$$\frac{d\sigma}{d\Omega} = \frac{\alpha^2\beta_p C(s)}{4s}\left(|G_M(s)|^2(1+\cos^2\theta_p) + \frac{4m_p^2}{s}|G_E(s)|^2\sin^2\theta_p\right),$$

where: m_p, β_p and θ_p are the outgoing proton mass, velocity and angle with respect to the incoming e^-, respectively, in the e^+e^- center-of-mass (CM) frame; $s = m^2_{p\overline{p}}$ is the squared CM energy; the Coulomb term $C(s) = \pi\alpha(1-e^{-\pi\alpha/\beta_p})/\beta_p$ leads to a nonzero value at threshold; and G_E and G_M are the electric and magnetic form factors of the proton. At threshold, the two form factors are expected to be equal in magnitude; at high s, G_E becomes invisible and G_M is expected to fall as $\alpha_s^2(s)/s^2$.

Experimentally, we measure the total cross section and the angular distribution of the final state proton. From the latter, we extract the ratio $|G_E/G_M|$, whereas the cross section is proportional to the "effective form factor" $F_p^2(s) = (|G_M(s)|^2 + [2m_p^2/s]|G_E(s)|^2)/(1+[2m_p^2/s])$. However, the angular distribution can be difficult to measure and affects the extraction of the cross section.

Previous measurements cover limited energy ranges and/or lack precision. They indicate an unexpected rise toward threshold ($s \to 4m_p^2$), which, together with a number of near-threshold enhancements in baryon-antibaryon mass spectra from various experiments, remains to be explained. At higher energies, there are quite precise measurements, but at only a few energies. Our previous result also indicates possible structure in the 2-3.5 GeV range.

2. The ISR process and event reconstruction

The *BABAR* experiment [3] recorded e^+e^- data at CM energies near 10.6 GeV. However, the initial e^+ or e^- sometimes emits an energetic, real photon, denoted $\gamma_{\rm ISR}$, before annihilating at a reduced CM energy, and the cross section for a process such as $e^+e^- \to \gamma_{\rm ISR}p\overline{p}$ can be related to the $e^+e^- \to p\overline{p}$ cross section at the reduced energy by a well known radiator function. Using ISR events, one can therefore measure the reduced-energy process over a wide range of energies in a single experiment.

Most ISR photons are emitted at small angles with respect to the $e^\pm$ beams and escape detection, but 10% are emitted within the acceptance of the *BABAR* calorimeter and can be reconstructed. If such a "tagged" photon is sufficiently energetic, then the $p\overline{p}$ system is also well contained in the detector and is boosted toward it, resulting in full angular acceptance and good resolution for energies all the way down to threshold. Untagged ISR, in which the $\gamma_{\rm ISR}$ is not detected, but inferred from the kinematics of the reconstructed $p\overline{p}$ system, is useful at higher energies, and we have an analysis in progress.

We select $e^+e^- \to \gamma_{\rm ISR}p\overline{p}$ events by requiring at least one reconstructed photon candidate with energy above 3 GeV in the CM frame and two oppositely charged tracks both well within the acceptance of the tracking and particle identification systems. The identification of both tracks

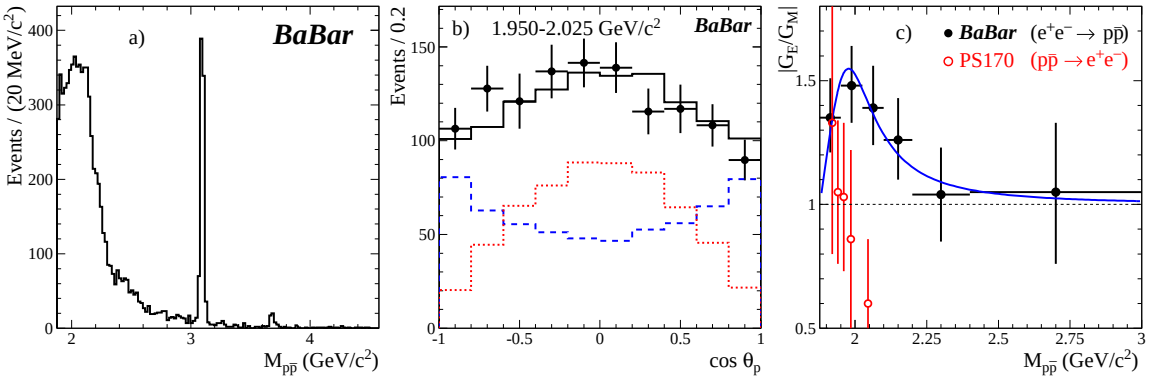

Figure 1: a) The $p\overline{p}$ invariant mass distribution for the selected $e^+e^- \to p\overline{p}$ sample. b) Background subtracted distribution of the polar angle of the proton with respect to the electron beam in the e^+e^- CM frame for events with $m_{p\overline{p}}$ in the range 1.95–2.025 GeV/c^2. The points represent the data, the dashed, dotted and solid lines represent the fitted $|G_M|$ and $|G_E|$ contributions and their sum, respectively. c) The ratio of electric to magnetic form factors extracted from this and similar fits in other $m_{p\overline{p}}$ regions.

as (anti)protons suppresses the backgrounds from $\gamma_{\rm ISR}K^+K^-$, $\gamma_{\rm ISR}\pi^+\pi^-$ and $\gamma_{\rm ISR}\mu^+\mu^-$ events by a factor of 10^4, while keeping 70% of the signal. A further ∼50-fold suppression is provided by a set of kinematic fits under various hypotheses. We require $\chi^2_{\gamma p\overline{p}} < 30$ and $\chi^2_{\gamma K^+K^-} > 30$, which retains 75% of the remaining signal. These backgrounds are cross-calibrated, along with the particle (mis)identification efficiencies, using the four event types and two suppression techniques, resulting in well understood backgrounds of at most 0.2%.

The invariant mass distribution for the selected events is shown in Fig. 1a, and is quite uniform from threshold up to 2.2 GeV/c^2. It then falls rapidly with energy, except for prominent J/ψ and $\psi(2S)$ peaks. The dominant background is from the process $e^+e^- \to p\overline{p}\pi^0$, in which an energetic π^0 is mistaken for a $\gamma_{\rm ISR}$. We evaluate this background from the data by combining the $\gamma_{\rm ISR}$ candidate with other photon candidates in the event and measuring the size of the π^0 peak. It amounts to 5.0±0.5% in the threshold region, and then grows with increasing energy to 50±20% at 4 GeV, limiting the measurement. Remaining backgrounds are evaluated from simulation and χ^2 control regions, and found to be small. We subtract the total estimated background in each bin.

3. Results

We study the angular distribution at the detector level in six ranges of $m_{p\overline{p}}$, as shown for a representative range in Fig. 1b. If $|G_E| = |G_M|$, then this distribution would be nearly uniform. We normalize simulated pure $|G_E|$ and $|G_M|$ contributions, shown as the dashed and dotted histograms, respectively, such that the total (solid histogram) best fits the data. The ratio $|G_E/G_M|$ extracted from each range is shown in Fig. 1c. It differs significantly from unity below 2.25 GeV/c^2, and is inconsistent with previous results from PS170. The curve is the result of a fit to an empirical function constrained to be unity at threshold and to approach unity asymptotically. A small forward-backward asymmetry is expected due to higher-order processes. We fit the $\cos\theta_p$ distribution for the combined range from threshold to 3 GeV/c^2 with an additional linear term, and obtain an asymmetry of -0.025 ± 0.014, consistent with both zero and a few-percent asymmetry.

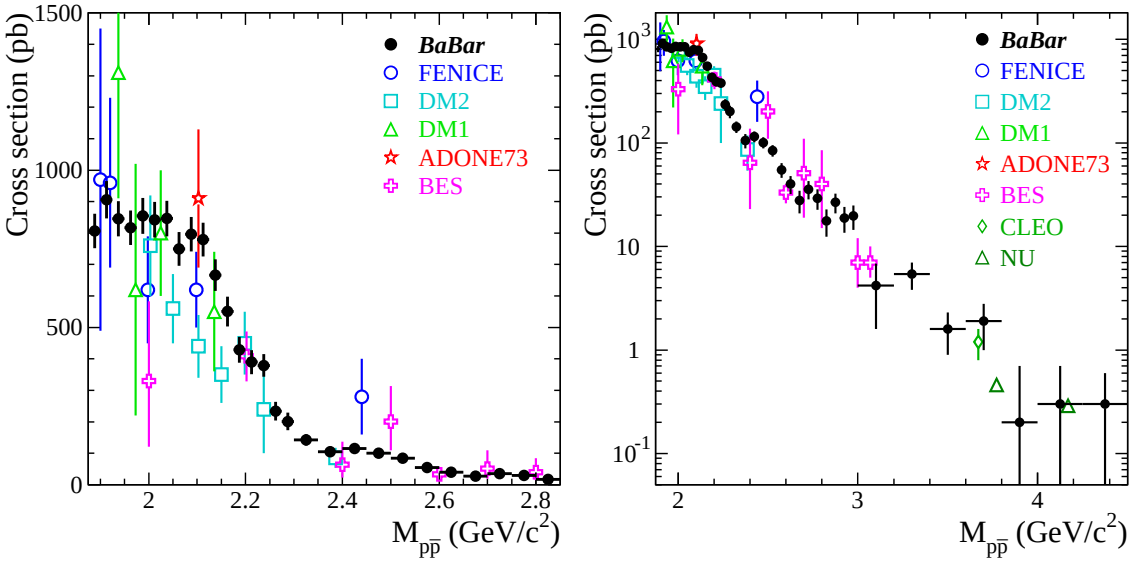

Figure 2: The $e^+e^- \to p\overline{p}$ cross section as a function of $m_{p\overline{p}}$, along with previous e^+e^- results. The two plots are identical, except for different $m_{p\overline{p}}$ ranges and linear (left) vs. logarithmic (right) vertical scales.

Our detection efficiency varies slowly with $m_{p\overline{p}}$, and is studied extensively in data and simulation. It is insensitive to $|G_E/G_M|$, and includes corrections to the simulation of up to 2%. The total uncertainty is 2.6% near threshold and drops slowly to 2.2% above about 3 GeV/c^2, dominated by contributions from the proton identification and $\gamma_{\rm ISR}$ reconstruction efficiencies.

We fit the J/ψ and $\psi(2S)$ peaks in the data, obtaining signals of 821±30 and 44±8 events, respectively. Correcting for efficiency and luminosity, we obtain the products of the electronic widths and branching fractions to $p\overline{p}$

$$\Gamma_{ee}^{1S} BF(J/\psi \to p\overline{p}) = 11.3 \pm 0.4 \pm 0.3 \quad \text{and} \quad \Gamma_{ee}^{2S} BF(\psi(2S)) \to p\overline{p}) = 0.67 \pm 0.12 \pm 0.13,$$

where the first error is statistical and the second systematic. Dividing by the PDG values of Γ_{ee}, we obtain competitive measurements of the branching fractions $BF(J/\psi \to p\overline{p}) = 2.04 \pm 0.10 \times 10^{-3}$ and $BF(\psi(2S) \to p\overline{p}) = 2.86 \pm 0.52 \times 10^{-4}$.

Excluding the J/ψ and $\psi(2S)$ signals, we extract the $e^+e^- \to p\overline{p}$ cross section as a function of $m_{p\overline{p}}$, shown in Fig. 3 with both linear (left) and logarithmic (right) vertical scales. All previous results from e^+e^- experiments are also shown, and are consistent. Our data cover a very wide range and are more precise except at the highest $m_{p\overline{p}}$ values. The cross section is very nearly uniform from threshold to 2.1 GeV/c^2, beyond which it drops rapidly with increasing $m_{p\overline{p}}$. there are indications of structure near 2.2, 2.5 and 3 GeV/c^2.

From this we calculate the effective form factor F_p, shown in Fig. 3 over two $m_{p\overline{p}}$ ranges. Also shown are previous e^+e^- results, as well as corresponding results from $p\overline{p}$ annihilation experiments. There is a rapid rise in F_p toward threshold; the shape of this rise in our data is consistent with that seen by PS170, but our results are higher overall by about 3σ. At higher masses, structures similar to those observed in the cross section are visible.

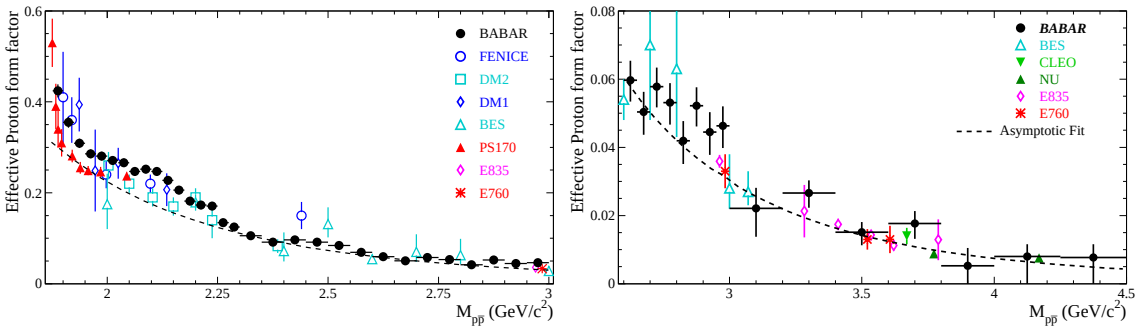

Figure 3: The effective proton form factor as a function of $m_{p\overline{p}}$, along with previous results. The two plots cover overlapping $m_{p\overline{p}}$ ranges. The lines represent the result of the QCD-motivated fit described in the text.

We test the asymtotic prediction of QCD by fitting the world's data above 3 GeV/c^2 with the function $f(m_{p\overline{p}}) = A\alpha_s^2(m_{p\overline{p}}^2)/m_{p\overline{p}}^{2n}$, where A and n are free parameters. The fit result, shown as the dashed lines on Fig. 3, is consistent with all data above 3 GeV/c^2, as well as with much of the lower-$m_{p\overline{p}}$ data. The fitted value of n is consistent with the predicted value of 2; A is not constrained theoretically, but is expected to be the same for spacelike and timelike form factors. The timelike values shown here are about twice the existing spacelike results in the 3–4.5 GeV/c^2 region.

4. Conclusion

In summary, we have measured the $e^+e^- \to p\overline{p}$ cross section from threshold to 4.5 GeV/c^2, and we have extracted J/ψ and $\psi(2S)$ braching fractions to $p\overline{p}$, the effective proton form factor over this range, and the electric:magnetic form factor ratio up to 3 GeV/c^2. This study uses our full data sample and supersedes our previous result.

Our measurements are consistent with most previous results, cover a wider range and are generally more precise. $|G_E/G_M|$ exceeds unity for $1.9 < m_{p\overline{p}} < 2.2$ GeV/c^2, and is inconsistent with the PS170 result from $p\overline{p}$ anihilation. The cross section is nonzero at threshold and nearly uniform just above threshold, and F_p shows the corresponding sharp rise toward threshold. Our results are consistent in shape with those from PS170, but differ in magnitude. These features remain to be explained, and any hypothesis must explain both F_p and $|G_E/G_M|$.

At high $m_{p\overline{p}}$, the data are consistent with the asymptotic form predicted by QCD. However, the existing time- and spacelike measurements are not consistent, so further measurements are needed at higher energies. In the intermediate $m_{p\overline{p}}$ region, there is evidence for structure near 2.2, 2.5 and 3 GeV/c^2 that needs to be explained.

References

[1] J.P. Lees, et al. (*BABAR* Collaboration), submitted to Phys. Rev. D.

[2] B. Aubert, et al. (*BABAR* Collaboration), Phys. Rev. D **73**, 012005 (2006).

[3] B. Aubert et al. (*BABAR* Collaboration), Nucl. Instr. Methods A **479**, 1 (2002); arXiv:1305.3560 [hep-ex], submitted to Nucl. Instr. Methods.